Friction **11**(2): 302–315 (2023)
https://doi.org/10.1007/s40544-022-0602-0
ISSN 2223-7690
CN 10-1237/TH
RESEARCH ARTICLE

A new mechanism for friction-induced vibration and noise

Fang CHEN[1], **Huajiang OUYANG**[2], **Xiaocui WANG**[3,*]

[1] *School of Automotive Engineering, Dalian University of Technology, Dalian 116024, China*

[2] *School of Engineering, University of Liverpool, Liverpool L24 9BF, UK*

[3] *College of Mechanical and Electrical Engineering, Wenzhou University, Wenzhou 325399, China*

Received: 10 June 2021 / Revised: 13 September 2021 / Accepted: 24 January 2022

Abstract: For years, friction-induced vibration and noise (FIVN) has puzzled many researchers in academia and industry. Several mechanisms have been proposed for explaining its occurrence and quantifying its frequencies, notably for automotive brake squeal, clutch squeal, and even rail corrugation. However, due to the complex and complicated nature of FIVN, there is not yet one fundamental mechanism that can explain all phenomena of FIVN. Based on experimental results obtained on a simple test structure and corresponding numerical validation using both complex eigenvalue analysis (CEA) and transient dynamic analysis (TDA), this study attempts to propose a new fundamental mechanism for FIVN, which is the repeated cycles of partial detachment and then reattachment of the contact surfaces. Since friction is ubiquitous and FIVN is very common, the insight into FIVN reported in this paper is highly significant and will help establish effective means to control FIVN in engineering and daily life.

Keywords: mechanism; friction-induced vibration and noise (FIVN); detachment; reattachment contact pressure

1 Introduction

Friction resists relative motion between two bodies in contact [1, 2]. Dry friction plays two seemingly paradoxical roles: Adds and dissipates energy. A friction system vibrates when it cannot dissipate all energy inputs, and such vibration is called friction-induced vibration (FIV), which is one kind of self-excited vibration [3–5]. Dry friction can generate sound, as in the well-known examples of singing glasses and string instruments, as well as all sorts of noise in brakes and clutches [3, 6]. Friction is ubiquitous, and friction-induced vibration and noise (FIVN) is very common in nature, our daily life, and industry [7–12]. Insects such as cicadas can generate loud noise by rubbing their wings [13]. Normally, FIVN is unwanted, as it reduces machining precision and surface finish quality of products, degrades actuation precision of robots, and creates noise pollution. Friction-induced noise is a big irritant—Floor creak in a dwelling is a nuisance to the residents, and brake noise has cost automotive industry a huge amount of warranty money.

Due to the complex and complicated nature of FIVN involving several disciplines, such as nonlinear dynamics, surface science, contact mechanics, tribology, and physical chemistry [14–17], this intriguing phenomenon has excited interests of generations of researchers for decades [18–23]. The fundamental mechanisms of FIVN seem particularly fascinating. Several mechanisms have been proposed to explain its causes. These include the well-known hypotheses of negative gradient of the coefficient of friction versus the relative velocity [14], stick–slip vibration [14], follower force [24], mode coupling [25], hammering [26], and the sprag–slip vibration [27]. Other theories include the moving couple [28] and feed-in energy [29].

These mechanisms can provide a physical explanation for FIVN under certain circumstances but a universal explanation is yet to be found. For stick–slip

* Corresponding author: Xiaocui WANG, E-mail: xcwang@wzu.edu.cn

vibration, there are two motion schemes: a stick regime in which the friction pair moves together and a slip regime in which there is relative motion between them. Such smooth motion could easily become unstable and then induce noise, but stick-slip vibration can only give a useful explanation for the FIVN at a low relative velocity [30, 31]. The sprag–slip vibration could explain the FIVN taking place in one direction of relative sliding, but not in the opposite direction [32]. The most commonly adopted FIVN mechanism for brake squeal is mode coupling, which has also been combined with other mechanisms [25]. In this hypothesis, two separate frequencies of the undamped friction-less system start to get close when the coefficient of friction increases, and eventually coalesce and their corresponding modes also become one when instability sets in Ref. [25]. Mode coupling was also adopted to explain the occurrence of rail corrugation [33] and train wheel polygonization. However, a number of observations have exposed its serious shortcomings for brake squeal. For example, one typical scenario is that the same brake system believed to be under the influence of mode coupling sometimes squeals and sometimes does not. On the other hand, a brake system with no mode coupling can also exhibit squeal phenomena. Therefore, an alternative (and even universal) FIVN mechanism is required, which is the motivation of this paper.

This paper attempts to offer an alternative and new explanation of the cause of FIVN, drawing on experimental observation and validated by numerical simulation. This new mechanism should be very useful as it will enable design and manufacture of machines that will possess a low noise signature and help mitigate FIVN. In this present paper, after setting the scene for the background of this study, experimental evidence is presented and analysed, in order to highlight the shortcomings of the mode-coupling mechanism and usher in a new and alternative mechanism for FIVN. Then a finite element model that simulates the experimental setup is described and numerical results from simulations of the experimental procedure are examined, which are found to agree quite well with the experimental observations and thus add strength to this new mechanism that it is the repeated events of partial loss of contact (detachment) and impact (reattachment) of the two bodies in sliding frictional contact that generate FIVN in many situations and largely during brake squeal.

2 Experimental

Mode-coupling has been used as a dominant mechanism to explain and model brake squeal, and other problems related to friction, for example rail corrugation [34]. It is the dominant mechanism in the Complex Eigenvalue Approach for these problems provided in ABAQUS [35] and is arguably the accepted squeal mechanism in automotive industry [36].

In order to verify the authors' view that friction-induced squeal is not fundamentally caused by mode coupling, a specially designed experiment is carried out. A rectangular steel plate with dimensions of 86.7 mm × 76.6 mm × 12.6 mm and mass of 648 g is used as the test plate. It sits on a block of foam in green and has three resonant frequencies measured at 5.7, 8.2, and 11.0 kHz in the measured frequency range from 4 to 12 kHz. A smaller steel block with dimensions of 43.0 mm × 25.3 mm × 12.6 mm and mass of 110 g is pushed to slide on the top surface of the steel plate by hand. The small block does not have any resonant frequency in the test frequency range and is considered to be a "rigid body" (it should be noted that the small block is not really a rigid body, here the "rigid body" simply means that the resonant frequencies of the small block are much higher than those of the steel plate), because of its size. Therefore, in this work, the well-separated measured resonant frequencies of the rectangular steel plate give the authors the initial confidence that such geometric dimensions should be good enough to verify whether the mode coupling will happen in the following research. These arrangements have guaranteed that there is no mode coupling could occur during squeal generation. This is intentional and is very important to prove the authors' argument. A thin film of foam with a smooth surface is attached to the bottom surface of this small block (referred to as the slider) to simulate the presence of the friction material in a real brake pad and facilitate the phenomenon of repeated detachment–reattachment cycles during the

sliding process. The surface of the steel plate is also polished to a nearly mirror-like finish to aid the same phenomenon. The sliding speed and contact pressure range in 0.001–0.02 m/s and 0.1–3.0 bar, respectively. The setup for a separate modal test of the test structure (when the slider is stationary) is illustrated in Fig. 1. In this figure, three accelerometers can be seen, and the small yellow spots are marks of wax used for attaching the accelerometers that are moved around to these places during a hammer test. The frequency response function obtained in the modal tests is given in Figs. 2–4.

During a squeal event, the sound signal is measured by a microphone at a distance of 100 cm away from the test structure. At the same time, the vibration is measured by an accelerometer on the steel plate. The frequency spectra from measured sound and acceleration are also illustrated in Figs. 2–4.

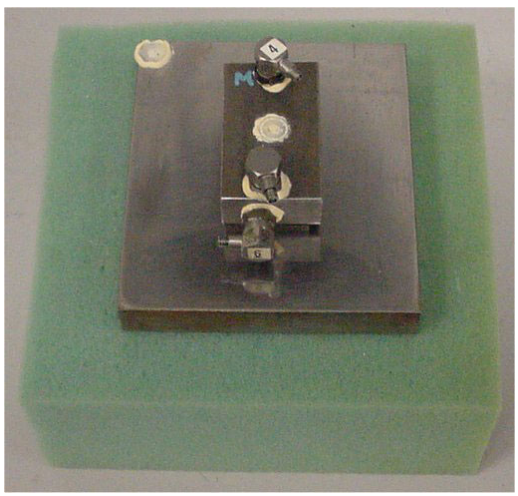

Fig. 1 Test setup for modal testing (using a hammer, which is not shown).

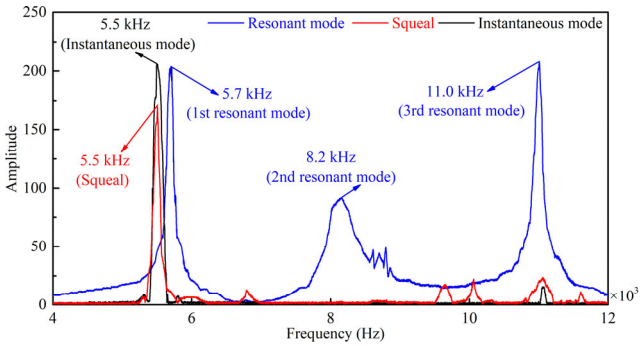

Fig. 2 Measured frequency spectra: sound signal (red solid line) and acceleration (dark solid line) during squeal of the whole structure, and free vibration of the steel plate (blue solid line).

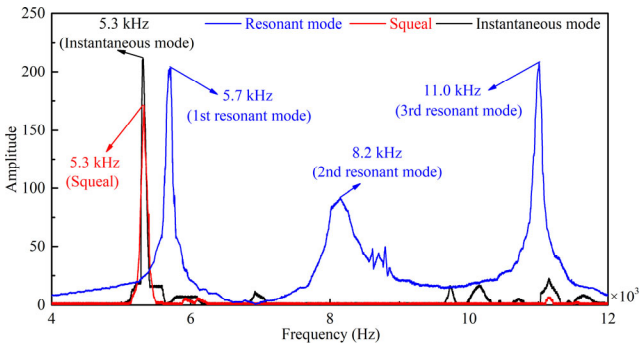

Fig. 3 Measured frequency spectra: sound signal (red solid line) and acceleration (dark solid line) during squeal of the whole structure, and free vibration of the steel plate (blue solid line).

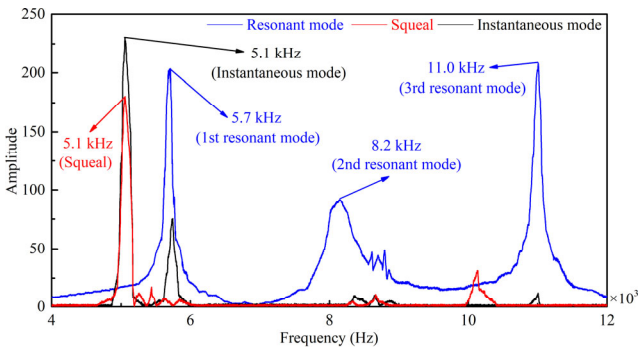

Fig. 4 Measured frequency spectra: sound signal (red solid line) and acceleration (dark solid line) during squeal of the whole structure, and free vibration of the steel plate (blue solid line).

The test results (some of which were report in Ref. [37]) can be summarised as follows:

1) It appears that squeal is not caused by mode coupling since not any two resonant frequencies of the steel plate are close enough for them to coalesce (please note that the steel block is much smaller and thus has much higher resonant frequencies than those of the steel plate, and the foam acts like a soft boundary).

2) A squeal frequency can be near one of the resonant frequencies, as shown in the tests.

3) In most cases, squeal frequencies (at 5.1, 5.3, and 5.5 kHz shown in Figs. 2–4) are lower than the first resonant frequency of 5.7 kHz of the steel plate. The differences between a squeal frequency and an adjacent resonant frequency can be more than 10% (5.1 kHz versus 5.7 kHz).

4) Figure 4 shows that the squeal frequency (5.1 kHz) is not directly related to the first resonant frequency of the steel plate at 5.7 kHz. On the other hand, a lower-intensity instantaneous mode occurs at 5.7 kHz.

5) Since squeal frequencies can be far away from and thus does not appear directly related to a resonant frequency, the corresponding squeal mode can be called an instantaneous squeal vibration mode or simply instantaneous squeal mode (ISM) or instantaneous mode as in Ref. [37]. In general, an ISM frequency is always aligned with a squeal frequency as shown in Figs. 2–4. In Figs. 2–4, the ISM frequencies are measured with an accelerometer attached at the test plate, and squeal frequencies are measured with a microphone near the test plate.

According to observation of the test results, the authors hypothesize that there are repeated cycles of detachment between the slider and the base plate and subsequent reattachment at the contact interface; and as the slider moves forward, these cycles of detachment and reattachment act like a periodic impulsive excitation and drive a transient wave around, which can explain the instantaneous nature of the squeal events, which is apparently not strongly related to a resonant frequency (of the base plate). This is believed to be what happens in real brake squeal events that have puzzled researchers for many years. Detachment at a contact interface and subsequent reattachment were found to be theoretically possible in moving-load problems involving frictional sliding [38].

3 Theoretical analysis

3.1 Mode-coupling instability

To demonstrate instability of friction-induced vibration in the form of mode coupling, a simple system shown in Fig. 5 below is analysed. The system consists of three masses with m_1 having a degree-of-freedom in x (horizontal) direction; m_3 having a degree-of-freedom in y (vertical) direction; and m_2 having degrees-of-freedom in both directions. m_1 is preloaded in compression and in sliding contact with a rigid belt moving at a constant speed via a massless rigid slider. The sliding friction at the slider–belt interface is governed by Coulomb friction whose static and kinetic friction coefficients are taken to be the same and the coefficient of friction is denoted by μ. There are 4 degrees-of-freedom (DoFs) in this system: horizontal and vertical displacements of m_2, which are

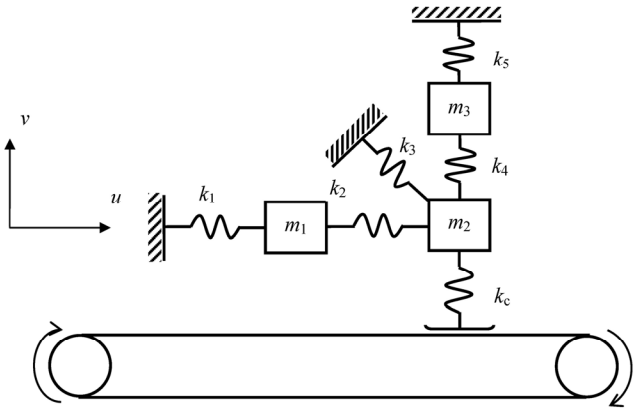

Fig. 5 4-DoF theoretical model.

u_2 and v_2; horizontal displacement of m_1, which is u_1; and vertical displacement of m_3, which is v_3.

The equation of motion can be derived as Eq. (1):

$$\boldsymbol{M}\ddot{\boldsymbol{x}} + \boldsymbol{K}\boldsymbol{x} = \boldsymbol{f} \tag{1}$$

where mass matrix $\boldsymbol{M}$ and stiffness matrix $\boldsymbol{K}$ are respectively,

$$\boldsymbol{M} = \begin{bmatrix} m_1 & 0 & 0 & 0 \\ 0 & m_3 & 0 & 0 \\ 0 & 0 & m_2 & 0 \\ 0 & 0 & 0 & m_2 \end{bmatrix}$$

$$\boldsymbol{K} = \begin{bmatrix} k_1 + k_2 & 0 & -k_2 & 0 \\ 0 & k_4 + k_5 & 0 & -k_4 \\ -k_2 & 0 & k_2 + 0.5k_3 & -0.5k_3 + \mu k_c \\ 0 & -k_4 & -0.5k_3 & k_4 + 0.5k_3 + k_c \end{bmatrix}$$

and displacement and force vectors are respectively,

$$\boldsymbol{x}^{\mathrm{T}} = \{u_1 \quad v_3 \quad u_2 \quad v_2\},\ \boldsymbol{f}^{\mathrm{T}} = \{0 \quad 0 \quad 0 \quad -N\}$$

in which N is the contact force due to the preload at the initial state of rest.

The linear stability of the system is characterised by the eigenvalues of the system, λ, in Eq. (2):

$$(\lambda^2 \boldsymbol{M} + \boldsymbol{K})\boldsymbol{\varphi} = 0 \tag{2}$$

Both λ and eigenvector $\boldsymbol{\varphi}$ are in general complex because of the friction-caused asymmetric term in matrix $\boldsymbol{K}$. If a system parameter is varied, the system eigenvalues (and their real and imaginary parts) vary with it. When these real and imaginary parts

are plotted against μ, bifurcation can be observed. In the following simulation, $m_i = 1$ kg$(i = 1,2,3)$, $k_i =$ 100 N/m$(i = 1,2,3,4,5)$, and $k_c = k_1$. The evolution of the eigenvalues is illustrated in Fig. 6.

It can be seen from Fig. 6 that two pairs of frequencies get closer as μ increases and they coalesce at $\mu = 1$, which indicates the two corresponding modes for each pair merge into one mode. At this point, their corresponding real parts of each pair start to bifurcate, beyond which one real part of each pair becomes positive and the system thus becomes unstable. This scenario of instability is called mode coupling. Similar phenomena happen to high-DoF systems, such as detailed finite element models of automotive brakes [39]. One important phenomenon which mode coupling fails to cover is the moving load effects [40].

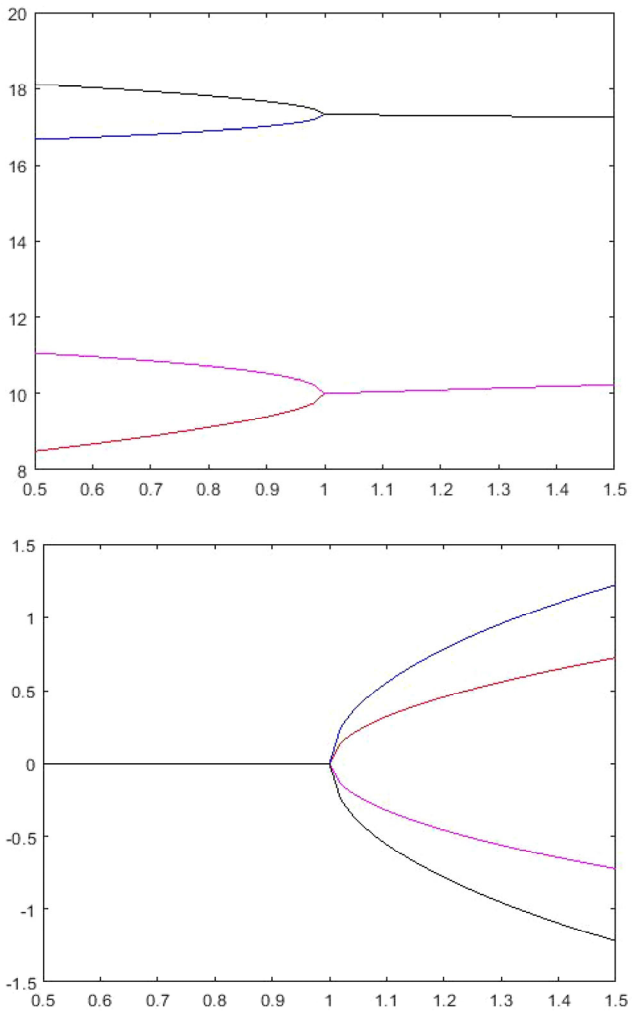

Fig. 6 Evolutions of the system eigenvalues with coefficient of friction. (a) Imaginary parts (frequencies) and (b) real parts (growth rates) versus coefficient of friction.

3.2 Finite element analysis

The purpose of this paper is to propose a new mechanism for generation of FIV. For this purpose, a 3-D finite element (FE) model is built in ABAQUS to simulate the tests described in Experimental Section, as shown in Fig. 7. The FE model includes the four key components of the real test structure: slider, film, steel plate, and foam. In this part, the modal analysis, the complex eigenvalue analysis (CEA), and the transient dynamic analysis (TDA) are reported. Firstly, the modal analysis is performed to validate the accuracy of the built FE model. Then, the CEA is made to verify through numerical methods that friction-induced squeal is not caused by mode coupling. Finally, the TDA is applied to study the dynamic behaviour of the model. The dimensions of each component are the same as those of the real test structure. The material properties of the components in the FE model are given in Table 1. It should be noted that the material properties of the slider and the steel plate are based on those of the real components, the material properties of the form and film in Table 1 may be higher than those of their true values, but various other values of them are used in the subsequent CEA to guarantee that the material parameters of foam and film will not alter the main conclusions of this paper. Furthermore, considering that the friction may lead to unstable vibration, the

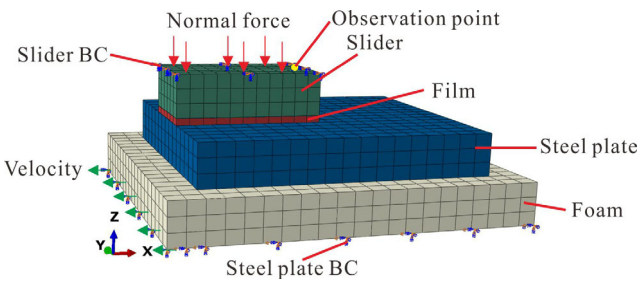

Fig. 7 FE model of the test structure.

Table 1 Material parameters of each component in the FE model.

Component	Density ρ (g/cm^3)	Young's modulus E (GPa)	Poisson's ratio ν
Steel slider	8.05	210	0.3
Film	1	10	0.25
Steel plate	7.74	230	0.28
Foam	1	10	0.25

damping of each component is set to zero deliberately to verify whether the friction in this structure causes mode-coupling instability and to support the proposed mechanism in this work.

Based on the real test structure, the boundary conditions (BC for short in Fig. 7) in the model are: the top surface of the slider is free in vertical z direction and fixed in other directions; the bottom surface of the foam is free in x direction and fixed in the other directions. A normal pressure (see the red arrows in Fig. 7) is applied onto the top surface of the slider, and an x-direction velocity (the green arrow in Fig. 7) is imposed to the bottom surface of the foam.

In this FE model, all the element type used is C3D8R (eight-node linear brick element with reduced integration) with advancing front meshing algorithm which can efficiently improve the quality of the mesh. Compared with other element types, C3D8R can efficiently reduce computational time and ensure good accuracy. A convergence analysis is performed before the proper numerical analysis to make sure that the built FE model is adequate for the CEA and TDA with good efficiency.

3.2.1 *Modal analysis*

Firstly, a modal analysis is conducted to verify the built FE model. The calculated natural frequencies of the steel plate are 5.7, 8.0, and 10.8 kHz in the frequency range from 4 to 12.0 kHz. Compared with the first three measured resonant frequencies of the steel plate (5.7, 8.2, and 11.0 kHz), the predicted and measured resonant frequencies (without friction) are very close, and therefore, the built FE model is thought to be reliable. Since the first resonant frequency from simulation (5.7 kHz) agrees very well with the first measured resonant frequency (5.7 kHz), the discussion in Section 3.2.3 is mainly focused around this frequency.

3.2.2 *CEA*

In the CEA, three cases are analysed to verify whether there appears mode-coupling instability when the slider is at different positions relative to the steel plate: the slider is at the starting position (Case 1, as shown in Fig. 8(a)); the slider is in middle (Case 2, as shown in Fig. 8(b)); the slider is at the end position (Case 3, as shown in Fig. 8(c)). The dynamic behaviour of the friction system is investigated at various values of the coefficient of kinetic friction, in the frequency range of 0–12 kHz, in keeping with the frequency range in the experiments.

The CEA results are shown in Tables 2–4, in the form of real parts and the imaginary parts (frequencies) versus the coefficient of friction. It can be seen that no mode coupling happens in any case, even at a very high value of coefficient of friction being 1.

3.2.3 *TDA*

In this part, the Dynamic Explicit solver is used to perform TDA. The automatic time step is used and the convergence of state variables at the end of a time step is not required. The TDA is about a dynamic contact problem with a moving contact interface, which is complicated to simulate, despite the simple geometric shapes of the components involved. The relative sliding velocity must be low enough to allow

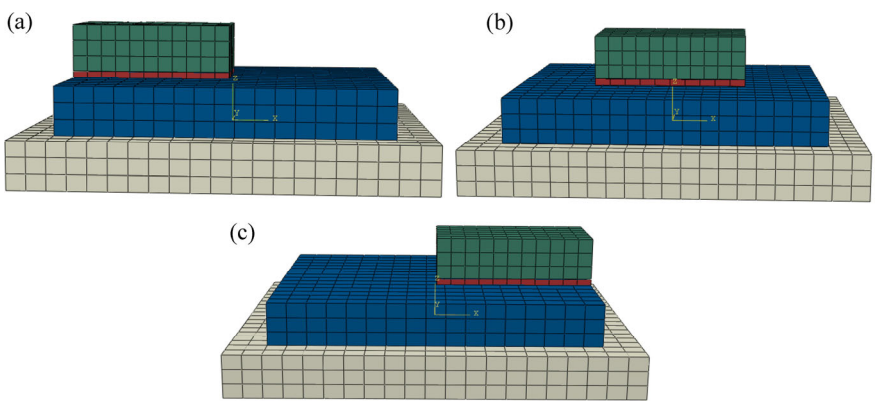

Fig. 8 Slider at various positions for CEA. (a) At the starting position (Case 1); (b) in the middle (Case 2); and (c) at the ending position (Case 3).

Table 2 CEA result for Case 1.

Model		$\mu = 0$	$\mu = 1$
Mode 1	Real part of eigenvalue	0	0
	Frequency (Hz)	9,455	9,841
Mode 2	Real part of eigenvalue	0	0
	Frequency (Hz)	9,478	10,012
Mode 3	Real part of eigenvalue	0	0
	Frequency (Hz)	10,601	10,947

Table 3 CEA result for Case 2.

Model		$\mu = 0$	$\mu = 1$
Mode 1	Real part of eigenvalue	0	0
	Frequency (Hz)	9,491	9,623
Mode 2	Real part of eigenvalue	0	0
	Frequency (Hz)	9,535	10,073
Mode 3	Real part of eigenvalue	0	0
	Frequency (Hz)	10,697	10,916

Table 4 CEA result for Case 3.

Model		$\mu = 0$	$\mu = 1$
Mode 1	Real part of eigenvalue	0	0
	Frequency (Hz)	9,455	8,355
Mode 2	Real part of eigenvalue	0	0
	Frequency (Hz)	9,477	9,739
Mode 3	Real part of eigenvalue	0	0
	Frequency (Hz)	10,601	10,855
Mode 4	Real part of eigenvalue	—	0
	Frequency (Hz)	—	11,277

contact between the slider and the base plate to be established but must not be too low for a simulation to take an exceedingly long time to finish. A sliding velocity of v = 3–10 mm/s is found to be a good compromise and also largely reproduces the main experimental observations. In ABAQUS, the normal pressure and the relative velocity are implemented gradually in the form of a ramp each to allow convergence of numerical simulations, as shown in Fig. 9. At first the normal pressure is applied and gradually increased until time t_1 = 0.1 s when it reaches the maximum of p = 0.1 MPa and then is kept at this constant level. The steel plate starts to slide at t_1 and the speed gradually increases up to time t_2 = 0.2 s when the velocity reaches the maximum (for example, v = 10 mm/s) and then remains constant.

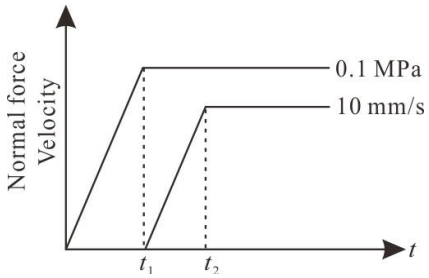

Fig. 9 Time history of the normal load and the sliding velocity of the steel plate.

In this investigation, a constant coefficient of (kinetic) friction, μ = 0.3 is used, which is obtained from the test. In this model, the film is in direct contact with the steel plate surface, and the surface-to-surface contact regime in ABAQUS is selected. The contact formulation is finite sliding with a penalty method, and the friction formulation is the simple Coulomb's law, while material damping and structural damping are neglected. The observation point (the yellow dot marked in Fig. 7) of the vibration acceleration is located on the surface of the slider, which is also where its acceleration is recorded in the experimental study. Based on the geometric dimensions of the steel plate and the slider, the total travelling time of the slider is set (for example, to be 4.37 s) to allow the slider to move from the left to the right along the steel plate for its left edge to reach the left edge of the steel plate.

Then a number of dynamic transient analyses are conducted to explore the dynamic behaviour of the FE model. Three examples are used to demonstrate typical vibration scenarios. One set of numerical results (Example 1) are shown in Figs. 10–12. Figure 10

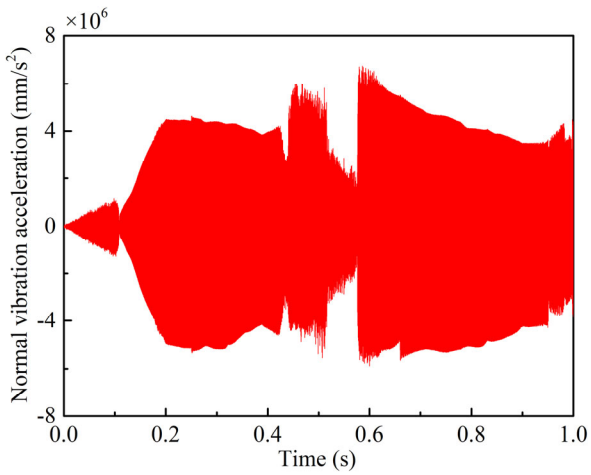

Fig. 10 Normal acceleration (v = 10 mm/s, p = 0.1 MPa).

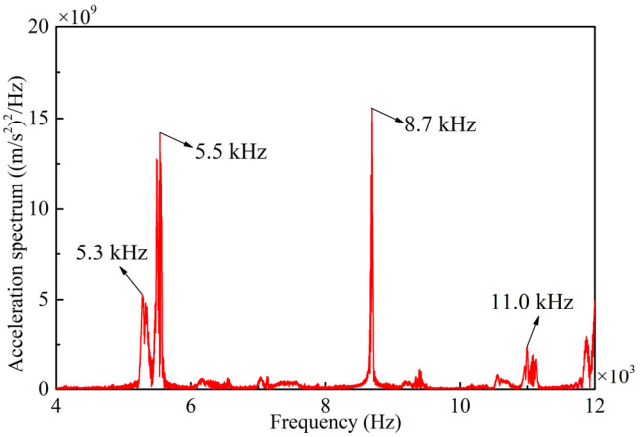

Fig. 11 Frequency spectrum for Fig. 10.

provides the time history of the normal acceleration at the observation point during the first 1 s duration of sliding. It can be found that the acceleration shows a complicated oscillation. Its corresponding frequency spectrum is given in Fig. 11, which displays several peaks, notably at 5.3, 5.5, and 8.7 kHz. Among them, 5.3 and 5.5 kHz agree very well with one set of the measured squeal frequency at 5.5 kHz (as shown in Fig. 2) and 5.3 kHz (as shown in Fig. 3). In addition, both these simulation and measured results of frequencies show that they are lower than the first measured (5.7 kHz) and theoretically predicted resonant frequency of 5.7 kHz of the steel plate obtained by simulation.

Figure 12 illustrates the evolution of the contact pressure at the slider–plate interface over time. The contact pressure is overall symmetrical about the longitudinal x axis. In the initial stage of sliding, the highest contact pressure concentrates on the leading edge (on the left), while the contact pressure on the trailing edge is almost zero, as shown in Figs. 12(a)–12(c). Although no detachment happens in this stage, energy is being added into the steel plate via friction and thus the vibration of the friction system grows. The contact pressure starts to show a very different distribution at 1.39 s with three pressure centres and the highest pressure shifts towards the trailing edge (on the right), as shown in Fig. 12(d); this shift of pressure is pronounced especially at 1.40 s, as shown in Fig. 12(e), while the contact pressure at the leading edge is almost zero, the distribution of which is opposite to the distribution during the initial stage. Then the highest contact pressure comes back to the leading edge, as shown in Figs. 12(g)–12(i).

As time goes on, the highest contact pressure moves to the trailing edge again, as shown in Figs. 12(j) and 12(l). Then there appears a new phenomenon—High contact pressure appears at/near both the leading and trailing edge, while the contact pressure in the middle is visibly low, as shown in Fig. 12(m). After this, the contact pressure distribution looks like a saddle, which is another unexpected phenomenon and can be seen in Fig. 12(n).

As the sliding continues, the position of the highest contact pressure shifts between the leading edge and trailing edge, as shown in Figs. 12(o)–12(t). Considering that the contact pressure distribution shows an approximately periodically shifting over the slider length, more oscillation cycles are not shown here.

It is important to observe that during sliding, the centre of contact pressure moves from left to right and back repeatedly and there are short periods of partial loss of contact (zero contact pressure). There are similar repeated events of detachment-reattachment, for example, during the period from 1.42 s, which are not shown to save space. They present a kind of periodic impulsive excitation that is believed by the authors to have induced the FIVN. The reattachments that happen in very short time durations act as impact which is known to be capable of exciting high-frequency vibration.

It should be noted that the detachment–reattachment may happen in other friction systems too. Li et al. [38] theoretically investigated the vibration of a 2-DoF slider rotating on the surface of annular disc and found the slider could separate from and then reconnect with the vibrating disc. The disc was modelled as plate which underwent only transverse vibration. Because the contact at the slider–disc interface was at one point, there was only a contact force. In contrast, the friction pair in this investigation is modelled as two three-dimensional deformable bodies and there is now contact area with time- and space-varying contact pressure.

It is also found from both experiments and numerical simulations that the occurrence of squeal and the frequency contents are sensitive to some operating conditions, i.e., the sliding speed and, in particular, the normal pressure. Figure 13 (Example 2) shows

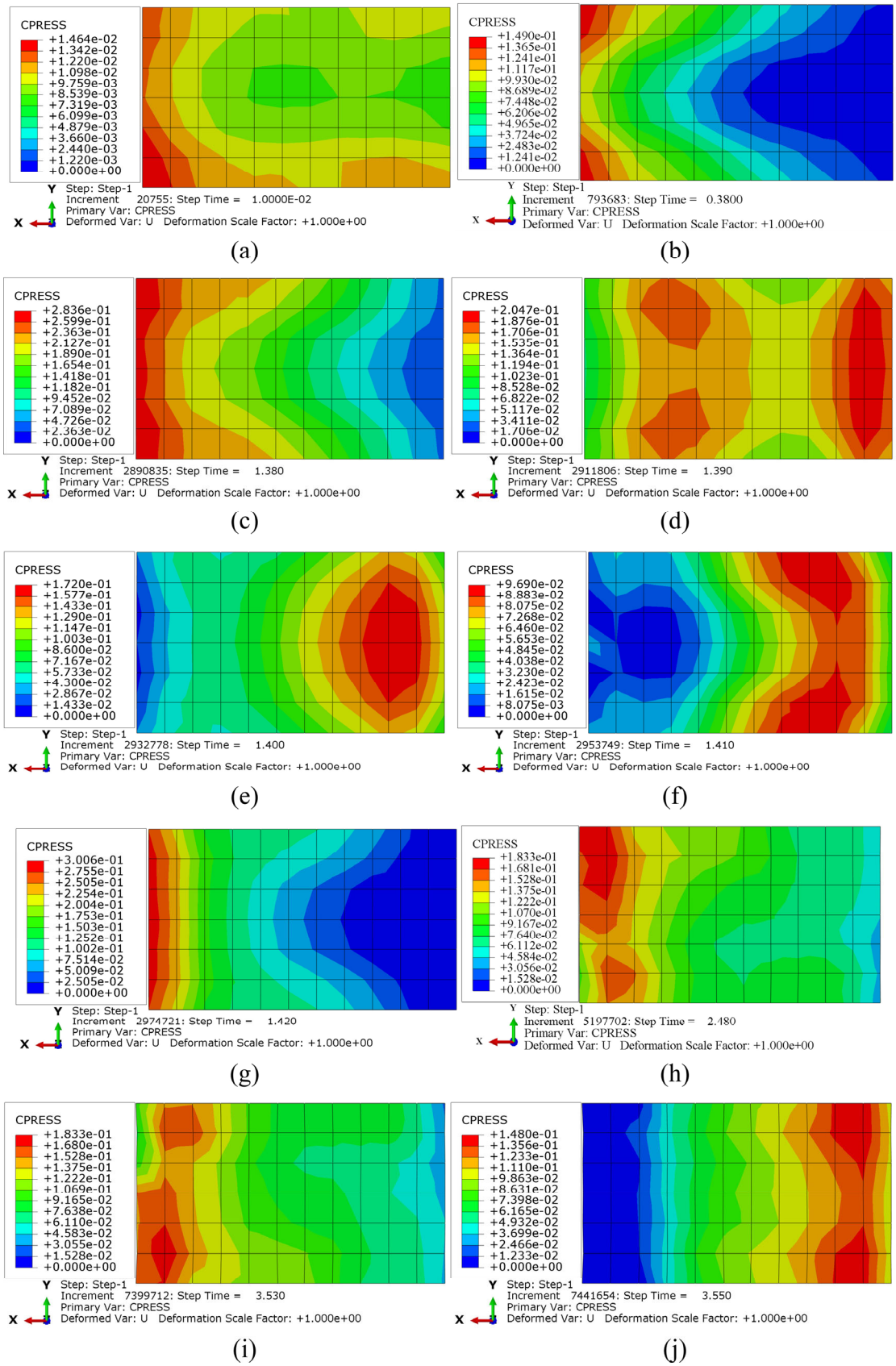

Fig. 12 Contact pressure distributions of film at different time instants.

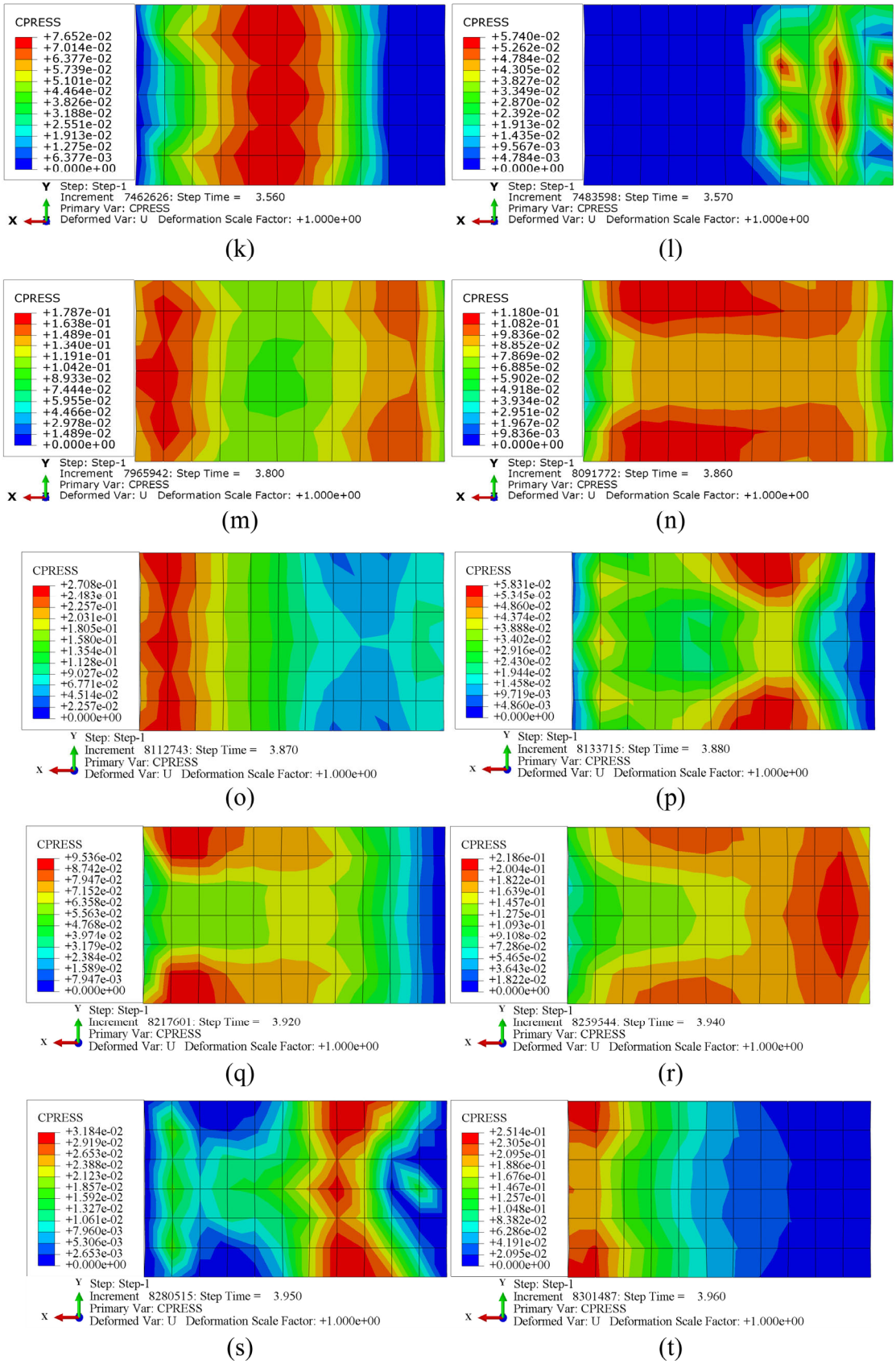

Fig. 12 (Continued)

the frequency spectrum of a numerical simulation in which the velocity is changed to 3 mm/s instead 10 mm/s as in the first example. Three similar dominant frequencies can be seen. Notably, the first frequency at 5.3 kHz in Fig. 11 now disappears and the frequency peak of 11.0 kHz becomes higher in this example, indicating a moderate dependence of instantaneous frequencies on the sliding velocity.

The frequency spectrum in Fig. 14 (Example 3) is obtained from a numerical simulation in which the velocity is 3 mm/s and the normal pressure is 0.3 MPa. Three different frequencies are seen to dominate the time-domain response. It should be highlighted that (1) the high frequency around 11.0 kHz now disappears, and (2) new frequencies (4.4, 4.6, 7.3, 7.5, 8.4, and 8.8 kHz) emerge, in which 4.4 and 4.6 kHz are near

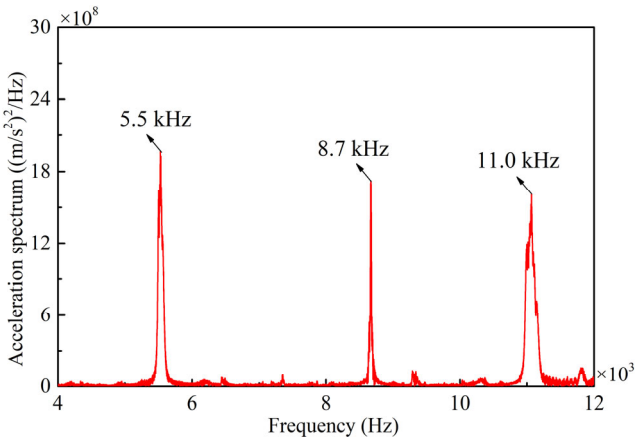

Fig. 13 Fast Fourier transform (FFT) spectrum of tangential acceleration (velocity: 3 mm/s; normal pressure: 0.1 MPa).

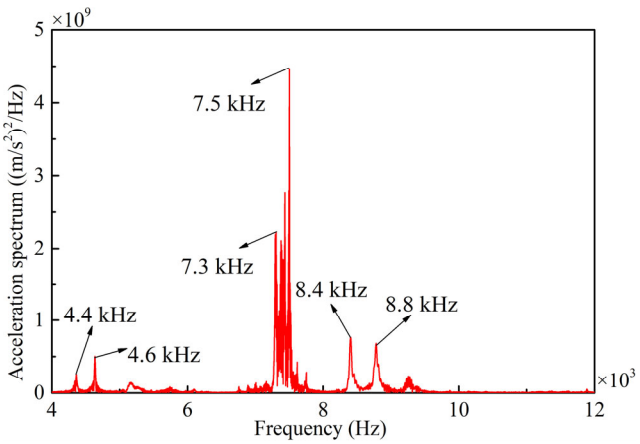

Fig. 14 FFT spectrum of tangential acceleration (velocity: 3 mm/s; normal pressure: 0.3 MPa).

and lower than the squeal frequency of 5.1 kHz measured in the experiments shown in Fig. 4. Due to the change of the normal pressure, a cluster of new frequencies between 7.3 and 7.5 kHz emerge and 7.5 kHz now becomes the dominant one in Fig. 14. Thus, it may be speculated that new frequencies in FIVN can emerge and the dominant frequency can vary when the operating conditions (for example, normal pressure and sliding speed) are proper. Actually, the results in Fig. 11 indicate that squeals can happen at many frequencies far away from resonant frequencies as long as the combination of sliding speed and contact pressure is proper. These further prove that squeal can happen even without the influences of resonant modes.

The simulation results in Fig. 14 and the previous test results show that squeal can occur at frequencies far away from the resonant frequencies of the main component (the steel plate) or the system. Thus, the periodic impulsive excitation caused by the repeated process of detachment–reattachment during friction sliding can be considered the dominant fundamental mechanism for squeal generation in this test structure and it is believed to be the dominant fundamental mechanism in brake squeal.

3.3 Short discussion of CEA and TDA results

CEA is based on the perturbed dynamic state around a static equilibrium point and is a linear dynamic stability analysis. In the experiments, the slider moves relatively to the steel plate and presents a moving distributed load, which makes the system time-variant. Therefore, CEA is not very suited to this kind of dynamic systems. Indeed, the frequencies from the CEA runs do not correlate well with the measured frequencies. More importantly, no (mode-coupling) instability is found in these CEA runs, which further indicates its capability of predicting FIV.

On the other hand, TDA tracks the relative movement of the slider and simulates the dynamic contact, and thus is better suited to simulate the experiments and other time-variant systems. Understandably, TDA takes much longer time than CEA for the problem solving under this study but it is worthwhile to do as it reveals phenomena that cannot be captured by CEA.

4 Conclusions

A combined experimental and theoretical study is conducted in this paper. In the experimental study, friction-induced-vibration (FIV) under various normal forces and sliding velocities is measured. In the theoretical study, the complex eigenvalue analysis (CEA) is applied to verify whether mode coupling will happen for this friction system, and transient dynamic analysis (TDA) is conducted to simulate the experimental procedure and study the vibration characteristics under different working conditions. The experimental and numerical results lead to the following conclusions:

1) From both TDA and experimental results, the values of main squeal frequencies are fairly sensitive to the sliding speeds and very sensitive to the normal contact pressures between the two bodies in sliding contact, even though the resonant/natural frequencies of the main component (the steel plate) and the system remain unchanged.

2) For the CEA results, no mode coupling is found in the friction system under study. TDA reveals that the pressure distribution at the contact interface shows (nearly) periodic time-varying patterns and the highest contact pressure changes its magnitude and position during sliding.

3) There appears a repeated process of detachment–reattachment of the friction pair at the contact interface during sliding, which provides a periodic impulsive excitation that is believed to be a foremost and fundamental mechanism of friction-induced vibration and brake squeal.

4) Squeal can be generated without mode coupling, and at frequencies even far away from the resonant frequencies, which confirms the authors' belief that squeal can be generated even without the influence of a resonant mode.

This work makes a significant contribution to understanding the FIVN and offers new thinking in reducing or exciting the FIVN in engineering and daily life, like controlling the detachment–reattachment of the brake pad and disc of an automobile brake system in order to impede and suppress unwanted FIVN.

Acknowledgements

The authors would like to thank Dr. Bowen Wu at Anhui Polytechnic University for providing the high-speed computer for the numerical study in this work. The support from the National Natural Science Foundation of China (No. 11672052) and Natural Science Foundation of Zhejiang Province (LQ22E050012) are gratefully acknowledged.

References

[1] Berger E. Friction modeling for dynamic system simulation. *Appl Mech Rev* **55**: 25–32 (2002)

[2] Kinkaid N M, O"Reilly O M, Papadopoulos P. Automotive disc brake squeal. *J Sound Vib* **267**: 105–166 (2003)

[3] Akay A. Acoustics of friction. *J Acoust Soc Am* **111**: 1525–1548 (2002)

[4] Rubino V, Rosakis A J, Lapusta N. Understanding dynamic friction through spontaneously evolving laboratory earthquakes. *Nat Commun* **8**: 15991 (2017)

[5] Ding C, Zhu H, Sun G D, Zhou Y K, Zuo X. Chaotic characteristics and attractor evolution of friction noise during friction process. *Friction* **6**(1): 47–61 (2018)

[6] Popp K, Stelter P. Stick–slip vibrations and chaos. *Philosophical Transactions of the Royal Society of London Series A* **332**: 89–105 (1990)

[7] Kendrick J E, Lavallée Y, Hirose T, Di Toro G, Hornby A J, De Angelis S, Dingwell D B. Volcanic drumbeat seismicity

caused by stick–slip motion and magmatic frictional melting. *Nat Geosci* **7**: 438–442 (2014)

[8] Papangelo A, Hoffmann N, Grolet A, Stender M, Ciavarella M. Multiple spatially localized dynamical states in friction-excited oscillator chains. *J Sound Vib* **417**: 56–64 (2018)

[9] Nicolas L A, Woodhouse J. Frequency measurement of musical instrument strings using piezoelectric transducers. *Vibration* **1**: 3–19 (2018)

[10] Woodhouse J, Lynch-Aird N. Choosing strings for plucked musical instruments. *Acta Acust united Ac* **105**: 516–529 (2019)

[11] Kruse S, Tiedemann M, Zeumer B, Reuss P, Hetzler H, Hoffmann N. The influence of joints on friction induced vibration in brake squeal. *J Sound Vib* **340**: 239–252 (2015)

[12] Wang X F, Mo J L, Ouyang H J, Xiang Z Y, Chen W, Zhou Z R. Simultaneous energy harvesting and tribological property improvement. *Friction* **9**(5):1275–1291 (2021)

[13] Merrell R C, Doarn C R. Cicadas: Signal-to-noise ratios and other thoughts. *Telemed E-Health* **18**: 403–403 (2012)

[14] Avramov K V. Chaotic frictional vibrations excited by a quasiperiodic load. *Int Appl Mech* **42**: 1071–1076 (2006)

[15] Massi F, Berthier Y, Baillet L. Contact surface topography and system dynamics of brake squeal. *Wear* **265**: 1784–1792 (2008)

[16] Dong X, Dykman M I, Chan H B. Strong negative nonlinear friction from induced two-phonon processes in vibrational systems. *Nat Commun* **9**: 3241 (2018)

[17] Eriksson M, Bergman F, Jacobson S. Surface characterisation of brake pads after running under silent and squealing conditions. *Wear* **232**: 163–167 (1999)

[18] Coudeyras N, Sinou J J, Nacivet S. A new treatment for predicting the self-excited vibrations of nonlinear systems with frictional interfaces: The constrained harmonic balance method, with application to disc brake squeal. *J Sound Vib* **319**: 1175–1199 (2009)

[19] Zhao X, Grbner N, Wagner U V. Avoiding creep groan: Investigation on active suppression of stick-slip limit cycle vibrations in an automotive disk brake via piezoceramic actuators. *J Sound Vib* **441**: 174–186 (2018)

[20] Wang X C, Mo J L, Ouyang H J, Wang D W, Chen G X, Zhu M H, Zhou Z R. Squeal noise of friction material with groove-textured surface: An experimental and numerical analysis. *J Tribol* **138**(2): 021401 (2016)

[21] Neis P D, Ferreira N F, Poletto J C, Matozo L T, Masotti D. Quantification of brake creep groan in vehicle tests and its relation with stick–slip obtained in laboratory tests. *J Sound Vib* **369**: 63–76 (2016)

[22] Hassan M Z, Brooks P C, Barton D C. The evaluation of disc brake squeal propensity through a fully coupled transient thermomechanical model. *P I MECH ENG D-J AUT* **227**: 361–375 (2013)

[23] Abu Bakar A R, Ouyang H, James S, Li L. Finite element analysis of wear and its effect on squeal generation. *P I MECH ENG D-J AUT* **222**: 1153–1165 (2008)

[24] Mottershead J E. Vibration and friction-induced instability in disks. *The Shock and Vibration Digest* **30**: 14–31 (1998)

[25] Hoffmann N, Fischer M, Allgaier R, Gaul L. A minimal model for studying properties of the mode-coupling type instability in friction induced oscillations. *Mech Res Commun* **29**: 197–205 (2002)

[26] Rhee S K, Tsang P H S, Wang Y S. Friction-induced noise and vibration of disc brakes. *Wear* **133**: 39–45 (1989)

[27] Spurr R T. A theory of brake squeal. *P I MECH ENG D-J AUT* **1961**: 33–52 (1961)

[28] Ouyang H, Mottershead J E. Dynamic instability of an elastic disk under the action of a rotating friction couple. *J Appl Mech* **71**: 753–758 (2004)

[29] Zhang Z, Oberst S, Lai J C S. A non-linear friction work formulation for the analysis of self-excited vibrations. *J Sound Vib* **443**: 328–340 (2018)

[30] Tonazzi D, Massi F, Culla A, Baillet L, Fregolent A, Berthier Y. Instability scenarios between elastic media under frictional contact. *Mech Syst Signal P* **40**: 754–766 (2013)

[31] Paliwal M, Mahajan A, Don J, Chu T, Filip P. Noise and vibration analysis of a disc brake system using a stick slip friction model involving coupling stiffness. *J Sound Vib* **282**: 1273–1284 (2005)

[32] Kang J, Krousgrill C M. The onset of friction-induced vibration and spragging. *J Sound Vib* **329**: 3537–3549 (2010)

[33] Chen G X, Zhou Z R, Ouyang H, Jin X S, Zhu M H, Liu Q Y. A finite element study on rail corrugation based on saturated creep force-induced self-excited vibration of a wheelset–track system. *J Sound Vib* **329**: 4643–4655 (2010)

[34] Wu B, Qiao Q, Chen G, Lv J, Zhu Q, Zhao X, Ouyang H. Effect of the unstable vibration of the disc brake system of high-speed trains on wheel polygonalization. *P I Mech Eng F-J Rai* **234**: 80–95 (2019)

[35] Bajer A, Belsky V, Li J Z. Combining a nonlinear static analysis and complex eigenvalue extraction in brake squeal simulation. *SAE International* 2003-01-3349 (2003)

[36] Ouyang H, Nack W, Yuan Y, Chen F. Numerical analysis of automotive disc brake squeal: A review. *International*

Journal of Vehicle Noise & Vibration **1**: 207–230 (2005)
[37] Chen F. Automotive disk brake squeal: An overview. *Int J Vehicle Des* **51**: 39–72 (2009)
[38] Li Z, Ouyang H, Guan Z. Friction-induced vibration of an elastic disc and a moving slider with separation and reattachment. *Nonlinear Dyn* **87**: 1045–1067 (2017)
[39] Nobari A, Ouyang H, Bannister P. Uncertainty quantification of squeal instability via surrogate modelling. *Mech Syst Signal Process* **60–61**: 887–908 (2015)
[40] Ouyang H, Mottershead J E. Dynamic instability of an elastic disk under the action of a rotating friction couple. *J Appl Mech* **71**: 753–758 (2005)

Fang CHEN. He received his BEng degree in 1982, MEng degree in 1985 from Dalian University of Technology, and Ph.D. degree in 1995 from Oakland University in USA. He is a visiting scholarship professor in the School of Automotive Engineering, Dalian University of Technology. His research fields focus on friction induced vibration and noise, and laser imaging technologies.

Huajiang OUYANG. He received his BEng degree in 1982, MEng degree in 1985, and Ph.D. degree in 1989 from Dalian University of Technology. He is a professor in the School of Engineering, University of Liverpool. He is also a Changjiang Scholarship Professor. His research interests include friction-induced vibration, moving-load dynamics, vibration based structural identification and energy harvesting, and vibration control.

Xiaocui WANG. She received her MEng degree in 2012 and Ph.D. degree in 2020 from Southwest Jiaotong University. She is a lecturer in the School of Mechanical and Electrical Engineering, Wenzhou University. Her research interests are friction induced vibration and noise, and tribology design.